Applicability of the Global Land Evaporation Amsterdam Model Data for Basin-Scale Spatiotemporal Drought Assessment

Khoshnazar, Ali ; Corzo Perez, Gerald A.; Diaz, Vitali

DOI
https://doi.org/10.1007/978-3-031-14096-9_10

Publication date
2023

Document Version
Final published version

Published in
Application of Remote Sensing and GIS in Natural Resources and Built Infrastructure Management

Citation (APA)
Khoshnazar, A., Corzo Perez, G. A., & Diaz, V. (2023). Applicability of the Global Land Evaporation Amsterdam Model Data for Basin-Scale Spatiotemporal Drought Assessment. In V. P. Singh, S. Yadav, K. K. Yadav, G. A. Corzo Perez, F. Muñoz-Arriola, & R. N. Yadava (Eds.), *Application of Remote Sensing and GIS in Natural Resources and Built Infrastructure Management: Water Science and Technology Library* (Vol. 105, pp. 197-215). (Water Science and Technology Library). https://doi.org/10.1007/978-3-031-14096-9_10

Chapter 10
Applicability of the Global Land Evaporation Amsterdam Model Data for Basin-Scale Spatiotemporal Drought Assessment

Ali Khoshnazar, Gerald Augusto Corzo Perez, and Vitali Diaz

Abstract Drought directly impacts the living organisms and environment, and thereby, its assessment is essential. Different drought indices require different data, which can be obtained based on models or in-situ measurements, demanding a significant amount of effort. Using remotely sensed (RS) data from satellites can facilitate this data acquisition. Nowadays, more and more satellite techniques are rising, highlighting the need to assess the accuracy of their data and the reliability of the results obtained employing them. The Wet-environment Evapotranspiration Precipitation Standardized Index (WEPSI) has shown good performance in drought monitoring and assessment, especially for agricultural purposes. This chapter employs the Global Land Evaporation Amsterdam Model (GLEAM) data to investigate its applicability in the Lempa River basin drought assessment using WEPSI. In this order, evaluated data obtained from the Water Evaluation and Planning system (WEAP) were used as the basis for comparison. Precisely, a comparison was made with GLEAM and WEAP-based data as well as WEPSI time series based on these two datasets. The results show relatively high similarity between these two datasets and calculated WEPSI drought indices. This validates the good performance of GLEAM-based data in drought monitoring and assessment based on WEPSI.

Keywords Remote sensing · GLEAM · Drought index · WEPSI · Drought assessment · Drought monitoring · Drought analysis · Agricultural drought · WEAP · Lempa River basin

A. Khoshnazar (✉) · G. A. Corzo Perez · V. Diaz
IHE Delft Institute for Water Education, Delft, The Netherlands
e-mail: ali.khoshnazaar@gmail.com

G. A. Corzo Perez
e-mail: g.corzo@un-ihe.org

V. Diaz
e-mail: v.diazmercado@tudelft.nl

V. Diaz
Water Resources Section, Delft University of Technology, Delft, The Netherlands

V. P. Singh et al. (eds.), *Application of Remote Sensing and GIS in Natural Resources and Built Infrastructure Management*, Water Science and Technology Library 105,
https://doi.org/10.1007/978-3-031-14096-9_10

10.1 Introduction

Water is the fundamental basis of biological organizations (Voeikov and Del Giudice 2009), and thereby, alterations in its availability directly impact the living organisms and environment. Drought is mostly related to the lack of water in a specific period of time, leading to a reduction in the precipitation and variation of other meteorological variables (Mishra and Singh 2010). During the past decades, the areas affected by drought are almost doubled worldwide, which has increased mortality and respiratory-related disease (Berman et al. 2021). This hazard is also one of the most important drivers of agricultural production drop and economic losses that alter human life quality (Zhang et al. 2021). Drought assessment that needs hydrometeorological data is one of the essential tasks in water planning and management (Mishra and Singh 2010). This data necessity is a concern for drought index selection. The required hydrometeorological data are usually obtained from models or in-situ measurements and requires a high deal of effort. Using remotely sensed data from satellites can facilitate this data acquisition and therefore resolve this challenge. Nowadays, more and more satellite techniques are rising, highlighting the need to assess the accuracy of their data and the reliability of the results obtained employing this data (Congalton 1991). Application of remote sensing (RS) data in drought calculation and assessment is one area that requires comprehensive attention concerning these discussed issues (Schellberg et al. 2008).

There already exist numerous drought indices in the literature. However, the application of RS-data, its accuracy, and eligibility are not widely studied in the calculation of these drought indices. Regarding the methodology for drought index calculation and identification of this phenomenon, the Palmer Drought Severity Index (PDSI) (Palmer 1965) was one of earlier attempts for agricultural purposes. Later, the Standardized Precipitation Index (SPI) (McKee et al. 1993) was introduced, which is one of the well-known drought indices working based on the precipitation data. In an attempt to address PDSI's drawback and make it a suitable index for comparing different regions, a so-called Self-Calibrated Palmer Drought Severity Index (scPDSI) (Wells et al. 2004) was developed. Additionally, for considering the role of frozen precipitation that was missed in PDSI, Shafer and Dezman (Shafer and Dezman 1982) introduced the Surface Water Supply Index (SWSI). The Standardized Precipitation Evapotranspiration Index (SPEI) (Vicente-Serrano et al. 2010) is another widely used index that incorporates the role of climate change in SPI's structure. Khoshnazar et al. (2021a) suggested the Wet-environment Evapotranspiration Precipitation Standardized Index (WEPSI) that works based on SPI's structure and suggests applying the wet evapotranspiration as the suitable water demand indicator.

Wei et al. (2021) used remotely sensed data to monitor drought dynamics in China, employing a number of drought indices, including SPI. Javed et al. (2021) used global remote sensing data to study agricultural and meteorological droughts over China by applying the Standardized Precipitation and Vegetation Water Supply

Index (SVSWI). Vicente-Serrano et al. (2018) used remote sensing data to calculate the global Standardized Evapotranspiration Deficit Index (SEDI).

It is worth noting that obtaining ET data that is present in the structure of several drought indices largely depends on modeling or other expensive attempts that may restrict its popularity. In this process of obtaining ET, RS approaches come in handy as a low-cost approach compared to traditional methods (Wen et al. 2021). Recently, a wide range of RS-based ET products [e.g., the Global Land Evaporation Amsterdam Model (GLEAM) (Martens et al. 2017)] have been developed globally and locally to complement the limited land surface coverage of the ground-based ET measurements (Wagle and Gowda 2019). RS-based ET data are used to monitor water use and assist in planning management. This ET data can be employed to simplify obtaining the values of this variable and, consequently, incorporating it in WEPSI drought index structure to improve drought monitoring accuracy compared with only precipitation-based drought indices (e.g., SPI) (Lu et al. 2019).

Khoshnazar et al. (2021a) showed that water shortage, and thereby, WEPSI could capture soil moisture status, and there is a relation between WEPSI and cereal production (Lewis et al. 1998). Hence, in this research, we have assessed droughts by applying WEPSI at the catchment scale and have used ET data calculated from a hydrological model, the Water Evaluation and Planning system (WEAP). We have further incorporated a global ET dataset, the GLEAM data, to analyze the suitability of the remotely sensed data for its use in WEPSI-based local drought assessments. This is the first attempt to use remotely sensed data in WEPSI's structure that has shown good performance in agricultural drought monitoring.

The remainder of this chapter is organized as follows. Section 10.2 describes the materials and methods that are used in this research. The next section illustrates the results and provides discussions on them. And the final section concludes the chapter.

10.2 Materials and Methods

In this section, we first explain our case study area. Then, we provide a brief description of the two models (WEAP hydrological model and GLEAM RS-based model) used to obtain the required data for WEPSI calculation. Afterward, the WEPSI calculation method is explained. The final part of this section is dedicated to the description of the experimental setup.

10.2.1 Case Study

In order to investigate the applicability of remote sensing data, we selected the Lempa River basin, which is the longest river in the Central American dry corridor (422 km). The river emanates in Guatemala, and its mouth is the Pacific Ocean in El Salvadorian territory. 85% of the Lempa River length streams in El Salvador (Hernández 2005).

A part of the river is located in Honduras as well (Fig. 10.1; Khoshnazar et al. 2021b). Around half of El Salvador's land is shared with the basin area, which is 17,790 km^2. The basin's daily average temperature, total annual precipitation, and yearly runoff are 23.5 °C, 1698 mm, and 19.21 $dm^3\ s^{-1}\ km^2$, respectively. The majority of El Salvadorian surface water and its people depend on the Lempa River basin. At the same time, the river is highly affected by droughts and other extreme events that decreased its quality and quantity (El Salvador's Ministry of Environment and Natural Resources (MARN) 2019b; Global Environment Facility 2020; Helman and Tomlinson 2018; Jennewein and Jones 2016).

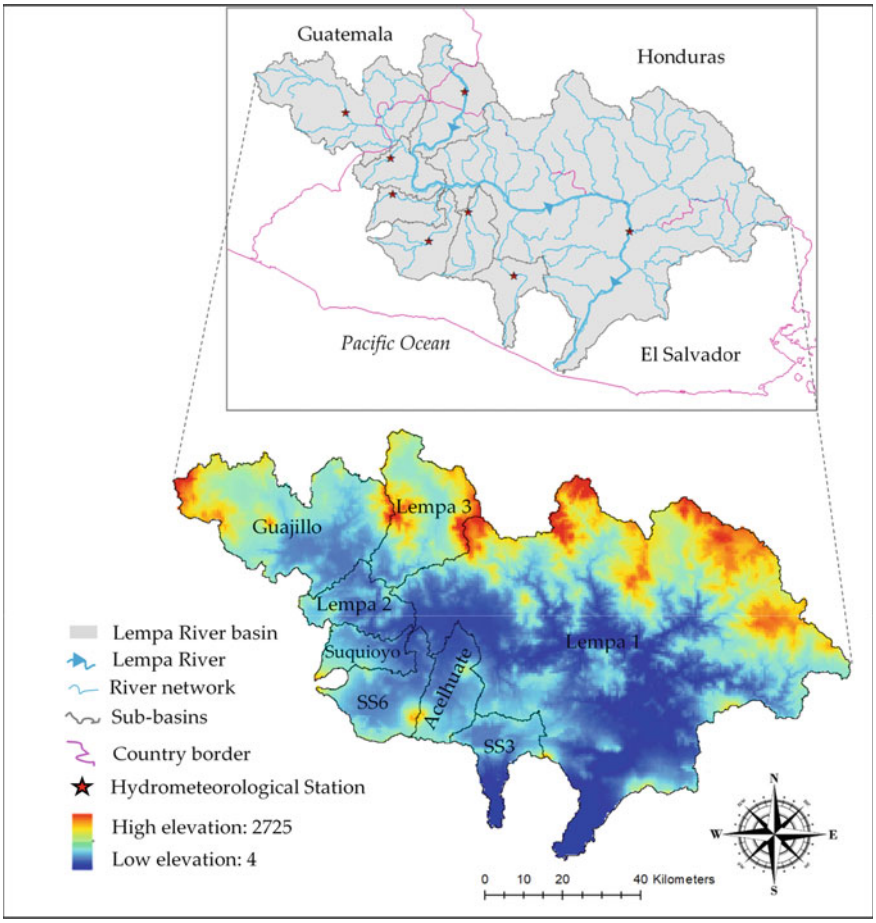

Fig. 10.1 Lempa river basin location (Khoshnazar et al. 2021b)

10.2.2 WEAP Model

The Stockholm Environment Institute's model 'the Water Evaluation And Planning system (WEAP)' (Seiber and Purkey 2015) is used to obtain essential data for WEPSI calculation between 1980 and 2010. El Salvador's Ministry of Environment and Natural Resources (MARN) (2020) data, including hydrometeorological and soil characteristics, were used as the model's inputs. The basin comprises eight sub-basins, including Lempa1, Lempa2, Lempa3, Guajillo, Suquioyo, Acelhuate, SS6, and SS3 (Fig. 10.1). The local management of the basin and its physiographic characteristics were the basis of this division.

Khoshnazar et al. (2021b) have shown that the WEAP-derived variables are reliable for drought assessment in the Lempa River basin. Our two previous papers describe more details of the validation and calibration procedure of the model (Khoshnazar et al. 2021a, 2021b). This is why we will refer to the WEAP-based WEPSI data as our actual data, hereafter called the observed data.

We selected the soil moisture method to simulate the basin processes like evapotranspiration (Fig. 10.2 shows the conceptual diagram for this method) (Seiber and Purkey 2015). In this model, the water balance is calculated by Eq. (10.1) as follows (Khoshnazar et al. 2021b; Oti et al. 2020) (assuming that the climate is steady in each sub-basin).

$$\mathrm{Rd}_j \frac{\mathrm{d}Z_{1,j}}{\mathrm{d}t} = P_\mathrm{e}(t) - \mathrm{ET_p}(t) k_{c,j}(t) \left(\frac{5Z_{1,j} - 2Z_{1,j}^2}{3} \right) - P_\mathrm{e}(t) Z_{1,j}^{\mathrm{RRF}_j} - f_j k_{s,j} Z_{1,j}^2 - \left(1 - f_j\right) k_{s,j} Z_{1,j}^2 \tag{10.1}$$

where $Z_{1,j}$ is the relative storage based on the total effective storage of the root zone. Rd_j is the soil holding capacity of the land cover fraction j (mm). $\mathrm{ET_p}$ is calculated using the modified Penman–Monteith reference crop potential evapotranspiration with the crop/plant coefficient ($k_{c,j}$). P_e is the effective precipitation, and RRF_j is the runoff resistance factor of the land cover. $P_\mathrm{e}(t) Z_{1,j}^{\mathrm{RRF}_j}$ is indicated as the surface runoff. $f_j k_{s,j} Z_{1,j}^2$ shows the interflow from the first layer, for which the term $k_{s,j}$ denotes the root zone saturated conductivity (mm/time); f_j is the partitioning coefficient that considers water horizontally and vertically, based on the soil, land cover, and topography. Finally, the term $\left(1 - f_j\right) k_{s,j} Z_{1,j}^2$ is percolation.

WEAP uses Eq. (10.2) to calculate $\mathrm{ET_a}$ (Khoshnazar et al. 2021b; Kumar et al. 2018).

$$\mathrm{ET_a} = \mathrm{ET_p} \frac{\left(5z_1 - 2z_2^2\right)}{3} \tag{10.2}$$

where z_1 and z_2 are the water depth of the top and bottom soil layers (bucket), respectively (Fig. 10.2).

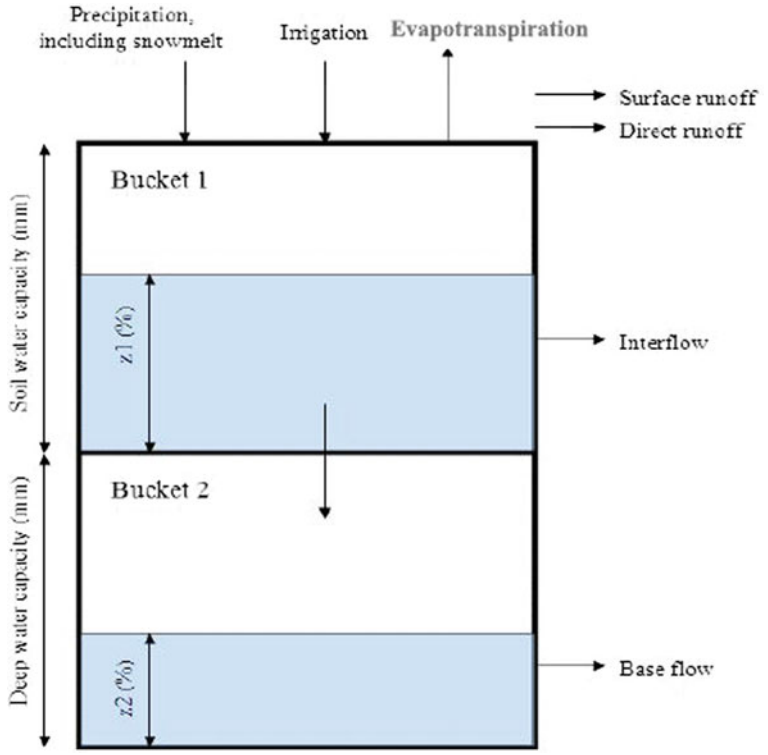

Fig. 10.2 Conceptual diagram of water balance calculation in WEAP (Seiber and Purkey 2015)

We calculated monthly ET_w with the WEAP-derived ET_p and ET_a following the procedure presented in Sect. 10.2.4.2. for each sub-basin.

10.2.3 GLEAM Data

The Global Land Evaporation Amsterdam Model (GLEAM) data provide ET_p and ET_a, among other variables (Martens et al. 2017; Miralles et al. 2011). We used the GLEAM v3.5a dataset in this research. This GLEAM version uses surface radiation and near-surface air temperature from the latest reanalysis of the European Center for Medium-Range Weather Forecasts (ECMWF)-ERA5, i.e., a combination of gauge-based reanalysis and satellite-based precipitation and vegetation optical depth. GLEAM datasets are provided within a monthly temporal.

We calculated the catchment-wide ET_p and ET_a for each sub-basin, where the actual and potential ET values of each sub-basin are obtained from the average values of all cells within the sub-basin on a monthly basis. Then, ET_w was computed with the procedure presented in Sect. 10.2.4.2.

10.2.4 The Wet-Environment Evapotranspiration and Precipitation Standardized Index (WEPSI)

10.2.4.1 WEPSI Calculation

As discussed, we have employed Wet-environment Evapotranspiration and Precipitation Standardized Index (WEPSI) for our drought assessment and monitoring. WEPSI is calculated as follows (Khoshnazar et al. 2021a): First, a long-term (at least 30 years) dataset of monthly water shortage (Eq. 10.3) is employed, and then, a time scale (aggregation period) is determined (can be 3, 6, 9, 12, 24, or 48 months). Then, the aggregated WS is fitted to a distribution function. In the next step, the cumulative probability function is equal to that of the normal distribution, for which the standardized variable with zero mean and unity standard deviation is obtained. As Khoshnazar et al. (2021a) suggest, we used the three-parameter log-logistic LL3 distribution to fit WS in WEPSI's calculation.

WS is the difference between precipitation (water supply) and wet-environment evapotranspiration (water demand) (Eq. 10.3).

$$\mathrm{WS} = P - \mathrm{ET_w} \tag{10.3}$$

Table 10.1 shows the drought categorical classification for WEPSI. This index categorizes the situation in eight classes, from extreme drought to extreme wet.

Table 10.1 Drought categorical classification using WEPSI (Khoshnazar et al. 2021a)

WEPSI value	Drought/wet category
≥2	Extreme wet
1.5 to 2	Severe wet
1 to 1.5	Moderate wet
0 to 1	Low wet
−1 to 0	Low drought
−1.5 to −1	Moderate drought
−2 to −1.5	Severe drought
≤−2	Extreme drought

10.2.4.2 ET_w Calculation

We used the methodology described by Khoshnazar et al. (2021a) for obtaining ET_w. As the reference suggested, a so-called complementary relationship (CR) is employed to relate ET_w, $ET_{p,}$ and ET_a. Kahler and Brutsaert (2006) suggested a general form for CR (Eq. 10.4).

$$(1+b)\,ET_w = bET_a + ET_p \tag{10.4}$$

where b is an empirical constant, ET_a, ET_p, and ET_w are actual, potential, and wet-environment evapotranspiration, respectively.

The symmetric CR considered by Bouchet is obtained by taking $b = 1$ in Eq. (10.4). However, the literature indicates that b generally exceeds and rarely is equal to 1, i.e., CR is asymmetric (Aminzadeh et al. 2016). Consequently, for the ET_w calculation, in addition to ET_p and ET_a, it is necessary to estimate the value of b.

Equation (10.4) can be rewritten in terms of b as follows (Aminzadeh et al. 2016).

$$b = \frac{ET_p - ET_w}{ET_w - ET_a} \tag{10.5}$$

Equation (10.5) shows that the increase of ET_p above the ET_w is proportional to the energy flux provided by surface drying and the decrease of evaporation rate. Normalizing Eq. (10.5) results in Eqs. (10.6) and (10.7) (Aminzadeh et al. 2016).

$$ET_{a+} = \frac{(1+b)\,ET_{MI}}{1+b\,ET_{MI}} \tag{10.6}$$

$$ET_{p+} = \frac{1+b}{1+b\,ET_{MI}} \tag{10.7}$$

where $ET_{a+} = \frac{ET_a}{ET_w}$, $ET_{p+} = \frac{ET_p}{ET_w}$, $ET_{MI} = \frac{ET_a}{ET_p}$, and ET_{MI} is the surface moisture index (with a maximum of 1). ET_{a+} and ET_{p+} are scaled actual and potential evapotranspiration, respectively.

To facilitate the calculation of the CR, Aminzadeh et al. (2016) suggested an atmospheric input-based equation for calculating b (Eq. 10.8).

$$b = AR_{S,net} + B \tag{10.8}$$

where $R_{S,net}$ is the net shortwave radiation flux in W m^{-2}. $R_{S,net}$ is calculated with the incoming shortwave radiation flux R_S and the surface albedo α as $R_{S,net} = (1-\alpha)R_s$.

A is a function of wind speed u_a (in m S^{-1}) (Eq. 10.9).

$$A = (3u_a + 2) \times 10^{-3} \tag{10.9}$$

Finally, the B parameter is calculated as a function of wind speed (u_a) and vapor concentration [c_a(kg m^{-3})] (Eq. 10.10).

$$B = (24.3u_a - 1.44)\left(c_a + 22 \times 10^{-3}\right) + 0.3 \tag{10.10}$$

To calculate b by Eq. (10.8), $R_{S,net}$, u_a, and c_a are required, which can be obtained from meteorological measurements, literature, or empirical equations. However, ET_w could be obtained from other sources or models. Khoshnazar et al. (2021a) proved that the mentioned methodology is more proper. As we do not confront data availability restrictions, we have followed their suggested path.

10.2.5 Experimental Setup

10.2.5.1 WEPSI Calculation at Catchment Scale

The implementation of the WEPSI drought indicator is investigated in the case study of the Lempa River basin. We estimated WEPSI for each of the river's sub-basins (Sect. 10.2.1). ET_w is calculated using Eq. (10.4). For each sub-basin, the b parameter is estimated using wind speed (u_a), net shortwave radiation $R_{S,net}$, and vapor concentration (c_a).

El Salvador's Ministry of Environment and Natural Resources (MARN) provided the meteorological data u_a, $R_{S,net}$, and c_a (El Salvador's Ministry of Environment and Natural Resources (MARN) 2019a). To calculate b, we first compute the monthly averages of u_a, $R_{S,net}$, and c_a for eight sub-basins. Then, we plug the values of each three input variables into Eq. (10.8) to get 12b values for each month and each sub-basin (Khoshnazar et al. 2021a).

We used the time series of WEAP-derived ET_p and ET_a (Sect. 10.2.2) as Eq. (10.4) inputs to determine ET_w in each sub-basin once b was calculated. Finally, we calculated WEPSI using the catchment-wide P and ET_w.

10.2.5.2 Eligibility of a Global Remotely Sensed ET Dataset for Local WEPSI Applications

In order to extend the use of WEPSI in other applications, it is necessary to have ET_w, which can be calculated through an approach similar to that presented in Sect. 10.2.2. Another option is through the use of global remotely sensed ET databases. In this sense, this part of the methodology is allocated to analyze the suitability of using global ET datasets to calculate WEPSI. The procedure involves two steps: (1) ET_w comparison and (2) the GLEAM-based WEPSI performance evaluation.

First, we extracted the catchment-wide ET_p and ET_a from the GLEAM dataset for each sub-basin. After that, we used the parameter b calculated in Sect. 10.2.4.2. to compute ET_w by Eq. (10.4). Then, we compared GLEAM- and WEAP-based ET_w by applying the following three commonly used metrics: the coefficient of determination (r^2), Kling-Gupta efficiency (KGE), and the percentage bias (PBIAS). The coefficient r^2 is calculated with Eq. (10.11).

$$r^2 = \left(\frac{\sum_{i=1}^{n}(x_i - \overline{x})(y_i - \overline{y})}{\sqrt{\sum_{i=1}^{n}(x_i - \overline{x})^2 \sum_{i=1}^{n}(y_i - \overline{y})^2}} \right)^2 \tag{10.11}$$

where x_i and y_i indicate the reference variable and the variable to compare, respectively, and $\overline{x}$ and $\overline{y}$ indicate the mean of each of them. KGE and PBIAS are obtained from Eqs. (10.12) and (10.13), respectively (Odusanya et al. 2019).

$$\mathrm{KGE} = 1 - \sqrt{(r-1)^2 + (\alpha - 1)^2 + (\beta - 1)^2} \tag{10.12}$$

$$\mathrm{PBIAS} = 100 \frac{\sum_{i=1}^{n}(x_i - y_i)}{\sum_{i=1}^{n} x_i} \tag{10.13}$$

where x_i and y_i indicate the reference variable and the variable to compare, respectively, α is the ratio between the standard deviation of the variable to compare and that of the reference variable ($\alpha = \sigma y / \sigma x$). Finally, β is the ratio between the mean of the variable to compare and that of the reference variable ($\beta = \overline{y}/\overline{x}$).

Second, after comparing ET_w, we calculated catchment-wide WEPSI with GLEAM-based ET_w. The difference between GLEAM- and WEAP-based WEPSI is the input ET_p and ET_a. With the time series of GLEAM-based WEPSI calculated in each sub-basin, we computed the time series of percentage of drought area (PDA) for the entire basin (Diaz et al. 2019). PDAs were calculated on a monthly basis as the ratio between the area of sub-basins in drought and the total area of the basin. A drought event starts once the drought index value comes below a threshold and ends as the value rises above the threshold again (Brito et al. 2018; Corzo Perez et al. 2011; Diaz et al. 2020). The threshold used in this application was drought index = −1, which is a threshold commonly employed in drought assessments (Diaz et al. 2020; Khoshnazar et al. 2021b).

10.2.5.3 Categorical Evaluation Statistics

Categorical validation techniques are vastly used for comparison or validating satellite data in the literature (Mayor et al. 2017; Sharifi et al. 2016; Yong et al. 2016). After calculating GLEAM- and WEAP-based WEPSI in the eight sub-basins, we employed three metrics using Table 10.2, as follows (Sharifi et al. 2016).

Table 10.2 Contingency table to evaluate drought occurrence by GLEAM data (Sharifi et al. 2016)

	GLEAM-based (estimated) drought			
WEAP-based (observed) drought		Yes	No	Total
	Yes	Hits (a)	Misses (c)	$a + c$
	No	False alarms (b)	Correct negative (d)	$b + d$
	Total	$a + b$	$c + d$	Total

The first applied categorical metric is the false alarm ratio (FAR), which indicates the fraction of estimated events that did not occur, and its ideal score is zero. FAR is calculated by Eq. (10.14).

$$\mathrm{FAR} = \frac{b}{a+b} \tag{10.14}$$

The second employed metric is the probability of detection (POD), which determines the fraction of the observed events correctly estimated. The best score of POD is one, and it is obtained from Eq. (10.15).

$$\mathrm{POD} = \frac{a}{a+c} \tag{10.15}$$

The third one is accuracy or fraction correct (FC), which measures the fraction of correct estimates, while its perfect score is one. FC is calculated using Eq. (10.16).

$$\mathrm{FC} = \frac{a+d}{\mathrm{total}} \tag{10.16}$$

10.3 Results and Discussion

10.3.1 WEPSI Calculation and Performance Evaluation

For the Lempa River basin, Khoshnazar et al. (2021a) have calculated parameter b in their research. They proved, compared to the symmetric CR, $b > 1$ leads to a considerable difference between the scaled evapotranspiration (ET_{a+} and ET_{p+}) as the surface dries and actual evapotranspiration decreases (Aminzadeh et al. 2016). They also highlighted the importance of using local meteorological data (net shortwave radiation, wind speed, and vapor concentration) that can lead to a better approximation of CR, and consequently, ET_w.

They also showed that WEPSI06 (i.e., WEPSI for the time step of 6 months) and SRI06 (i.e., SRI for the time step of 6 months) are most related in terms of low flows in the basin. Accordingly, they consider WEPSI06 as the representative of the

agricultural and hydrological drought conditions in the basin that means WEPSI06 reflects a realistic vision of the basin that links meteorological, agricultural, and hydrological drought. Accordingly, we employed WEPSI06 in our investigation to check the GLEAM data applicability.

10.3.2 Eligibility of a Global ET Dataset for Local WEPSI Applications

As discussed, we considered the WEAP-based data as our observed data. Figure 10.3a–c displays the r^2, KGE, and |PBIAS| between the GLEAM- and WEAP-based ET_w in the eight sub-basins of the Lempa River basin, respectively. As Fig. 10.3a shows, r^2 is more than 0.65 in the whole Lempa River basin. KGE satisfies the values larger than 0.5 all over the region, while more than 60% of the area has KGE $>$ 0.55. On the other hand, |PBIAS| is lower than 16% among the whole basin, while more than 60% of the area has a value lower than 10%.

Two sub-basins (Lempa2 and Suquioyo) have a value between 10 and 15%, and just Guajillo sub-basin has a value higher than 15% (but lower than 16%), which means the PBIAS results are acceptable (Odusanya et al. 2019).

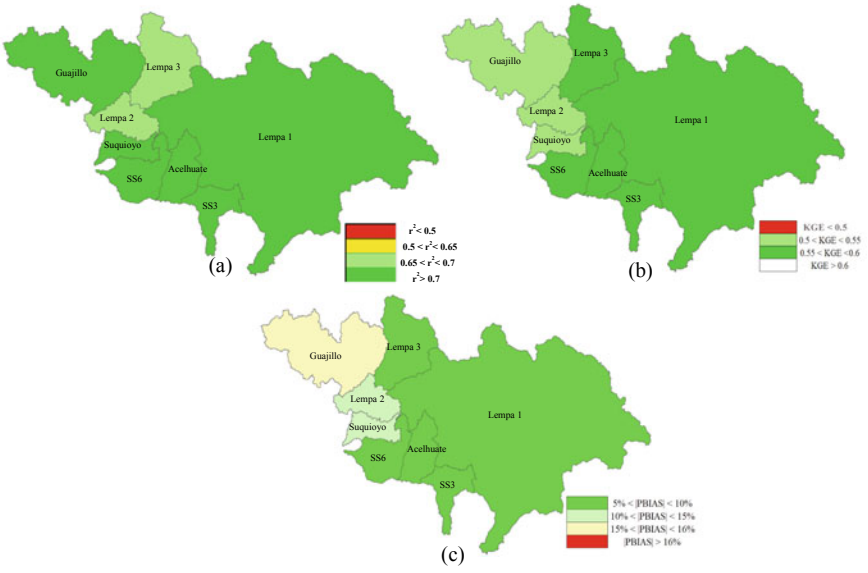

Fig. 10.3 Comparison of GLEAM- and WEAP-based ET_w in the sub-basins of Lempa River basin: **a** the coefficient of determination (r^2); **b** the Kling-Gupta efficiency (KGE); and **c** the percentage bias (PBIAS)

Generally, results depict that GLEAM-based ET_w is relatively similar to WEAP-based ET_w based on the three performance metrics, which indicates that GLEAM-based ET_w data can be used for local WEPSI applications (Odusanya et al. 2019). Results show that the GLEAM ET dataset can facilitate the global computation of WEPSI, where the lack of data is not a limitation and modeling is not required.

Figure 10.4a–h compares the time series of GLEAM- and WEAP-based WEPSI06 in the eight sub-basins of the Lempa River basin for the period 1980–2010 (31 years).

In general, the time series of both WEPSI06 are similar. Figure 10.4 concludes that for the GLEAM-based WEPSI06, the longest drought (i.e., the number of months that the value of WEPSI is below the threshold of −1) occurs in 2003, in general. The maximum drought frequency (3.54%) occurs in Guajillo, SS6, and Suquioyo sub-basins, with 13 total numbers of droughts over 31 years. The most severe drought (i.e., the aggregation of WEPSI values in sequent months at drought) occurs in Guajillo in December of 1994. These results that are obtained using the threshold of −1 as the onset of drought are similar to Khoshnazar et al. (2021a) investigation, which is based on WEAP data.

Figure 10.5 depicts WEAP- and GLEAM-based drought identification and differences between the two datasets in the eight sub-basins [a sub-basin is in drought if WEPSI06 ≤ 0 (Table 10.1)]. The employed threshold for drought onset (i.e., 0) provides more details about differences and consequently is a more suitable measure for accuracy assessment (compared to other lower thresholds, e.g., −1).

These data are used to obtain the three categorical metrics over the sub-basins (Table 10.3).

Table 10.3 contains amounts of categorical metrics as well as the mean elevation of each sub-basin. As the results suggest, Guajillo and Lempa3 have the highest values of POD and FC, respectively. These sub-basins have the highest average of elevation as well. On the other hand, Lempa2, which has the lowest mean elevation, faces the lowest values of POD and FC simultaneously.

FAR values do not show a direct relationship with the mean elevation of sub-basins. Among the eight sub-basins, Acelhuate and Lempa1 send the lowest false alarms, while SS6 and SS3 send more false alarms of drought based on GLEAM datasets.

Figure 10.6 displays the variation of drought areas through the PDAs in the Lempa River basin (whole area) for the overall 31 years based on GLEAM- and WEAP-based WEPSI06. The threshold of 0 was used to calculate drought in each WEPSI time series too.

As the figure shows, using the zero threshold as the onset of drought concludes the majority of times with the availability of drought. However, usually, the threshold of −1 is employed to this order, which provides more sensible results (Khoshnazar et al. 2021b). We have used our threshold to capture more phenomena for the comparison and therefore calculate more reliable continuous and categorical metrics for eligibility of GLEAM-based data. The result shows a correlation more significant than 0.85 between GLEAM- and WEAP-based PDA in November, February, July, August, and September. This is while March, April, and December have the lowest correlation coefficient values (all values are bigger than 0.6).

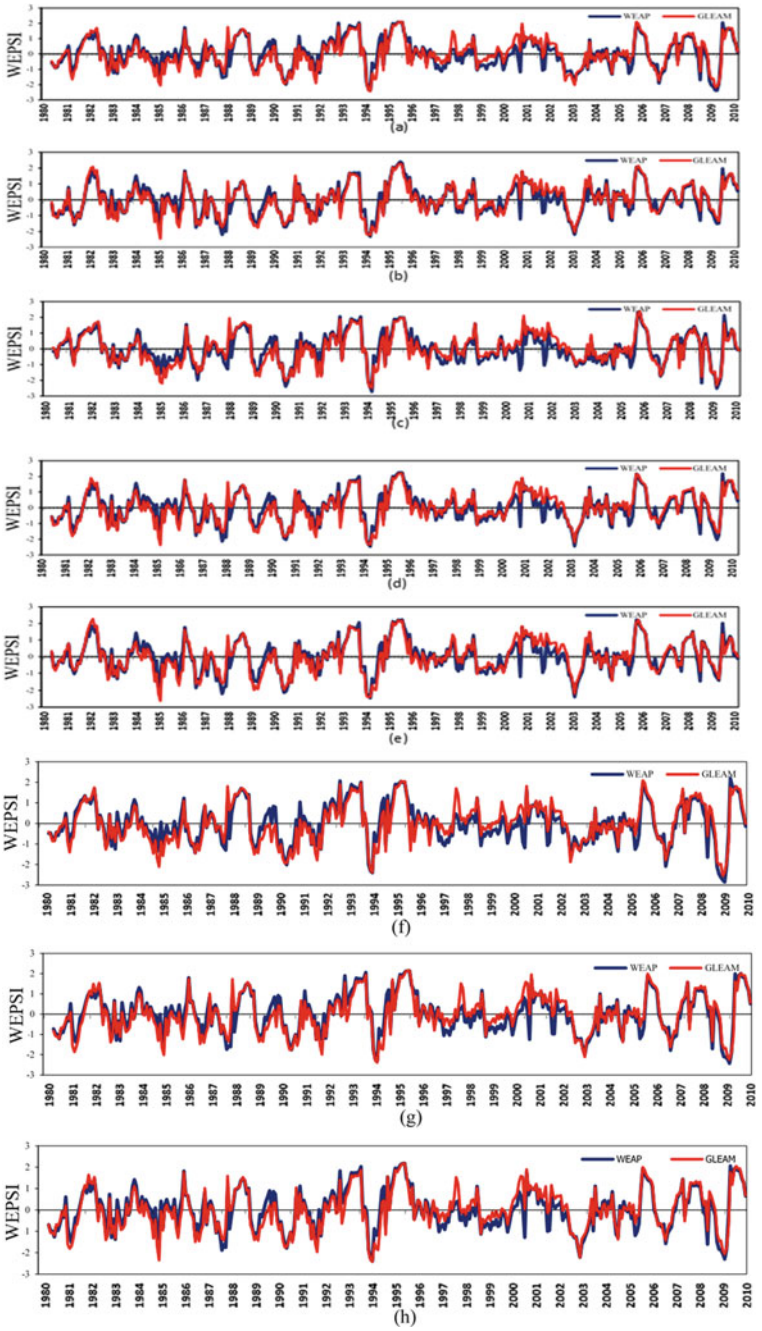

Fig. 10.4 Annual time series of GLEAM- and WEAP-based WEPSI06 in the sub-basins. **a** Acelhuate, **b** Guajillo, **c** Lempa1, **d** Lempa2, **e** Lempa3, **f** SS3, **g** SS6, and **h** Suquioyo

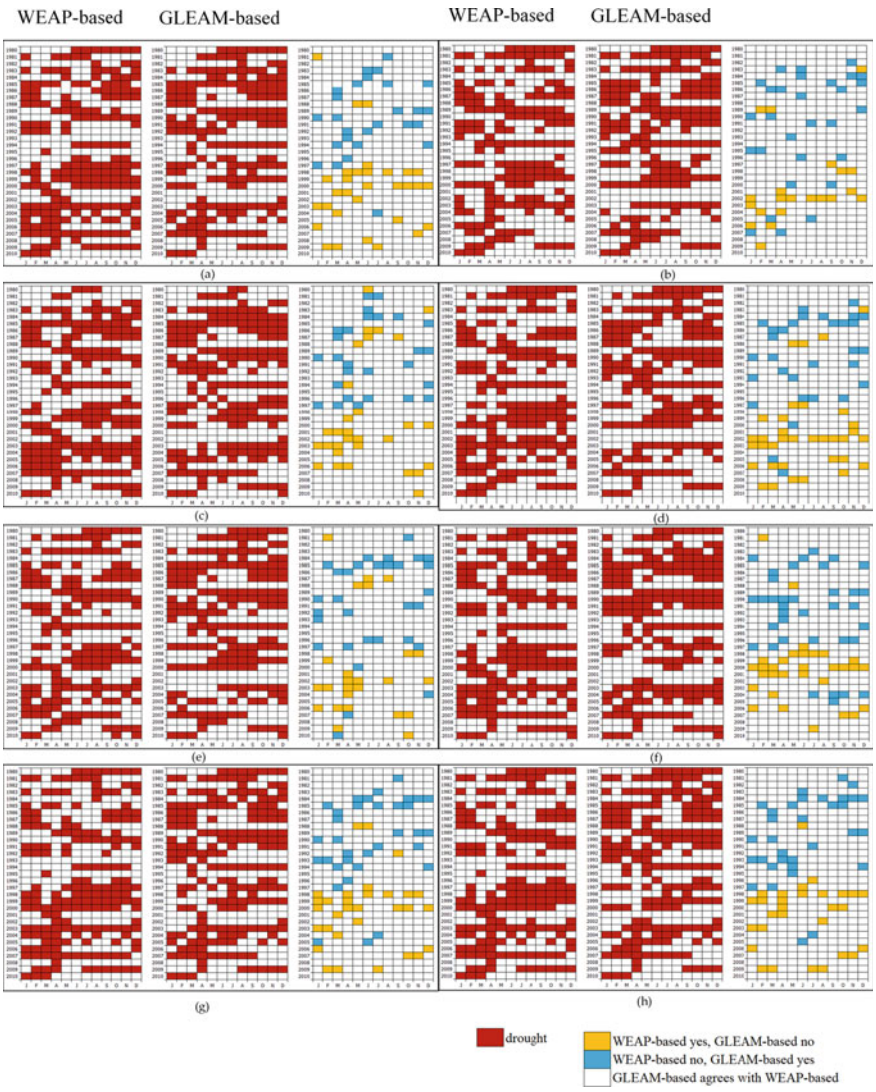

Fig. 10.5 WEAP- and GLEAM-based drought identification (i.e., WEPSI06 ≤ 0) and their differences, in the eight sub-basins: **a** Acelhuate, **b** Guajillo, **c** Lempa1, **d** Lempa2, **e** Lempa3, **f** SS3, **g** SS6, and **h** Suquioyo (The figure illustrates the situation of each sub-basin in 12 months of the year from 1980 to 2010. The situation is either white if two datasets are the same, blue if just the GLEAM-based ET_w determines a drought, or yellow if just the WEAP-based ET_w determines a drought. The red cells identify a drought)

Table 10.3 FAR, POD, and FC categorical metrics, and mean elevation of eight sub-basins

	FAR	POD	FC	Mean elevation (masl)
Acelhuate	0.15	0.84	0.84	585
Guajillo	0.16	0.88	0.86	926
Lempa1	0.15	0.84	0.84	775
Lempa2	0.17	0.81	0.82	505
Lempa3	0.17	0.86	0.85	1162
SS3	0.19	0.84	0.82	540
SS6	0.18	0.83	0.82	616
Suquioyo	0.17	0.84	0.83	574

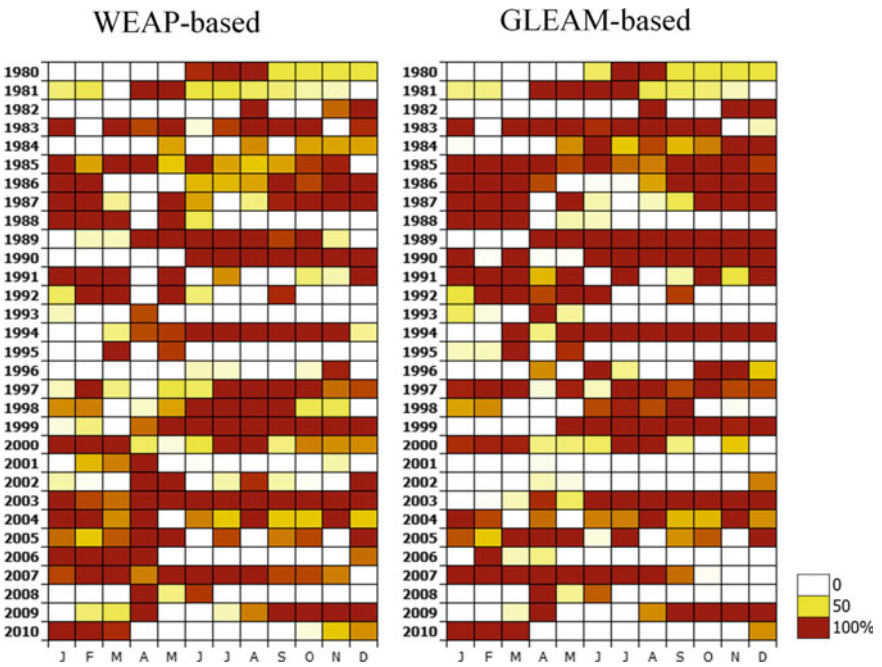

Fig. 10.6 Percentage of drought area (PDA) employing WEPSI06 based on GLEAM and WEAP data in the Lempa River basin from 1980 to 2010

August and September also have the lowest percentage of mean absolute error between the two compared PDAs (3.9 and 5.4%, respectively), while March and April face the highest percentage of mean absolute error (11.1 and 12.4%, respectively).

Obtaining evapotranspiration from classic methods or simulations is usually computationally expensive, as it needs many inputs such as hydrometeorological, soil, and vegetation data. Global RS ET datasets can resolve the challenge of retrieving ET data. Further evaluation that includes more basins and other global

ET databases is required. However, based on the results, a good performance is expected from WEPSI.

10.4 Conclusions

The Wet-environment Evapotranspiration and Precipitation Standardized Index (WEPSI) was employed in this study, which takes water shortage (WS) as its input. Precipitation (P) and wet-environment evapotranspiration (ET_w) are used to calculate WS. WEPSI was put to the test in the Lempa River basin, Central America's longest river.

For modeling with the Water Evaluation and Planning system (WEAP), the basin is divided into eight sub-basins. ET_w is calculated using WEAP's ET_p and ET_a. In order to facilitate WEPSI's application in other basins, we tested a global ET dataset for ET_w calculation. We used the Global Land Evaporation Amsterdam Model (GLEAM) ET_p and ET_a to calculate ET_w. GLEAM- and WEAP-based ET_w were compared with r^2, the Kling-Gupta efficiency (KGE), and the percentage bias (PBIAS). As the categorical metrics, we also used probability of detection (POD), false alarm ratio (FAR), and fraction correct (FC). The metrics reflect an acceptable similarity between these two datasets. Additionally, GLEAM- and WEAP-based WEPSI shows considerable similarities. These results indicate that WEPSI can be used in combination with global ET datasets for local drought assessments. Employing remotely sensed data (e.g., GLEAM), WEPSI could be calculated worldwide and under various climates and can provide a spatial and temporal depiction of drought variation.

Finally, drought events calculated with GLEAM-based WEPSI were compared. Results indicate that WEPSI that is also helpful for agricultural drought assessments (Khoshnazar et al. 2021a) could be calculated using GLEAM-based data.

This research's outcomes come in handy for the researchers and policymakers in drought calculation, monitoring, risk assessment, and forecasting. As a future research direction, we suggest using remote sensing-based WEPSI in other case studies and with other purposes.

Acknowledgements Authors thank the grant No. 2579 of the Albert II of Monaco Foundation. VD thanks the Mexican National Council for Science and Technology (CONACYT) and Alianza FiiDEM for the study grand 217776/382365.

Author Contributions A.K.: conceptualization, methodology, investigation, data processing, validation, software, writing—original draft; G.A.C.P.: conceptualization, project administration, supervision, review; V.D.: conceptualization, methodology, data processing, writing—review and editing. All authors have read and agreed to the published version of the manuscript.

References

Aminzadeh M, Roderick ML, Or D (2016) A generalized complementary relationship between actual and potential evaporation defined by a reference surface temperature. Water Resour Res 52(1):385–406

Berman JD, Ramirez MR, Bell JE, Bilotta R, Gerr F, Fethke NB (2021) The association between drought conditions and increased occupational psychosocial stress among US farmers: an occupational cohort study. Sci Total Environ 149245

Brito SSB, Cunha APM, Cunningham C, Alvalá RC, Marengo JA, Carvalho MA (2018) Frequency, duration and severity of drought in the Semiarid Northeast Brazil region. Int J Climatol 38(2):517–529

Congalton RG (1991) A review of assessing the accuracy of classifications of remotely sensed data. Remote Sens Environ 37(1):35–46

Corzo Perez G, Van Huijgevoort M, Voß F, Van Lanen H (2011) On the spatio-temporal analysis of hydrological droughts from global hydrological models. Hydrol Earth Syst Sci 15(9):2963–2978

Diaz V, Corzo G, Van Lanen HA, Solomatine DP (2019) Spatiotemporal drought analysis at country scale through the application of the STAND toolbox. In: Spatiotemporal analysis of extreme hydrological events. Elsevier, Amsterdam, pp 77–93

Diaz V, Perez GAC, Van Lanen HA, Solomatine D, Varouchakis EA (2020) An approach to characterise spatio-temporal drought dynamics. Adv Water Resour 137:103512

El Salvador's Ministry of Environment and Natural Resources (MARN). https://marn.gob.sv/. Retrieved 21 Sept 2019

El Salvador's Ministry of Environment and Natural Resources (MARN). Water resources maps. https://web.archive.org/web/20090422151648; http://snet.gob.sv/cd2/SeccionSIG/map_hi.htm. Retrieved 16 Dec 2019

El Salvador's Ministry of Environment and Natural Resources (MARN). https://marn.gob.sv/. Retrieved 14 June 2020

Global Environment Facility. https://www.thegef.org/project/fostering-water-security-trifinio-region-promoting-formulation-tdasap-its-transboundary. Retrieved 1 Sept 2020

Helman P, Tomlinson R (2018) Two centuries of climate change and climate variability, East Coast Australia. J Mar Sci Eng 6(1):3

Hernández W (2005) Nacimiento y Desarrollo del río Lempa. MARN/SNET

Javed T, Zhang J, Bhattarai N, Sha Z, Rashid S, Yun B, Ahmad S, Henchiri M, Kamran M (2021) Drought characterization across agricultural regions of China using standardized precipitation and vegetation water supply indices. J Clean Prod 127866

Jennewein JS, Jones KW (2016) Examining 'willingness to participate' in community-based water resource management in a transboundary conservation area in Central America. Water Policy 18(6):1334–1352

Kahler DM, Brutsaert W (2006) Complementary relationship between daily evaporation in the environment and pan evaporation. Water Resour Res 42(5)

Khoshnazar A, Perez GAC, Diaz V, Aminzadeh M (2021a) Wet-environment evapotranspiration and precipitation standardized index (WEPSI) for drought assessment and monitoring. Earth Space Sci Open Archive 25

Khoshnazar A, Corzo Perez GA, Diaz V (2021b) Spatiotemporal drought risk assessment considering resilience and heterogeneous vulnerability factors: Lempa transboundary river basin in the central American dry corridor. J Mar Sci Eng 9(4):386

Kumar P, Masago Y, Mishra BK, Fukushi K (2018) Evaluating future stress due to combined effect of climate change and rapid urbanization for Pasig-Marikina River, Manila. Groundw Sustain Dev 6:227–234

Lewis J, Rowland J, Nadeau A (1998) Estimating maize production in Kenya using NDVI: some statistical considerations. Int J Remote Sens 19(13):2609–2617

Lu Z, Zhao Y, Wei Y, Feng Q, Xie J (2019) Differences among evapotranspiration products affect water resources and ecosystem management in an Australian catchment. Remote Sens 11(8):958

Martens B, Miralles DG, Lievens H, Schalie RVD, De Jeu RA, Fernández-Prieto D, Beck HE, Dorigo WA, Verhoest NE (2017) GLEAM v3: satellite-based land evaporation and root-zone soil moisture. Geosci Model Dev 10(5):1903–1925

Mayor YG, Tereshchenko I, Fonseca-Hernández M, Pantoja DA, Montes JM (2017) Evaluation of error in IMERG precipitation estimates under different topographic conditions and temporal scales over Mexico. Remote Sens 9(5):503

McKee TB, Doesken NJ, Kleist J (1993) The relationship of drought frequency and duration to time scales. In: Proceedings of the 8th conference on applied climatology, Boston, pp 179–183

Miralles DG, Holmes T, De Jeu R, Gash J, Meesters A, Dolman A (2011) Global land-surface evaporation estimated from satellite-based observations. Hydrol Earth Syst Sci 15(2):453–469

Mishra AK, Singh VP (2010) A review of drought concepts. J Hydrol 391(1–2):202–216

Odusanya AE, Mehdi B, Schürz C, Oke AO, Awokola OS, Awomeso JA, Adejuwon JO, Schulz K (2019) Multi-site calibration and validation of SWAT with satellite-based evapotranspiration in a data-sparse catchment in southwestern Nigeria. Hydrol Earth Syst Sci 23(2):1113–1144

Oti JO, Kabo-Bah AT, Ofosu E (2020) Hydrologic response to climate change in the Densu River Basin in Ghana. Heliyon 6(8):e04722

Palmer WC (1965) Meteorological drought. US Department of Commerce, Weather Bureau, p 30

Schellberg J, Hill MJ, Gerhards R, Rothmund M, Braun M (2008) Precision agriculture on grassland: applications, perspectives and constraints. Eur J Agron 29(2–3):59–71

Seiber J, Purkey D (2015) WEAP—water evaluation and planning system user guide for WEAP. Stockholm Environment Institute

Shafer B, Dezman L (1982) Development of surface water supply index (SWSI) to assess the severity of drought condition in snowpack runoff areas. In: Proceeding of the western snow conference

Sharifi E, Steinacker R, Saghafian B (2016) Assessment of GPM-IMERG and other precipitation products against gauge data under different topographic and climatic conditions in Iran: preliminary results. Remote Sens 8(2):135

Vicente-Serrano SM, Beguería S, López-Moreno JI (2010) A multiscalar drought index sensitive to global warming: the standardized precipitation evapotranspiration index. J Clim 23(7):1696–1718

Vicente-Serrano SM, Miralles DG, Domínguez-Castro F, Azorin-Molina C, El Kenawy A, McVicar TR, Tomás-Burguera M, Beguería S, Maneta M, Peña-Gallardo M (2018) Global assessment of the standardized evapotranspiration deficit index (SEDI) for drought analysis and monitoring. J Clim 31(14):5371–5393

Voeikov V, Del Giudice E (2009) Water respiration-the basis of the living state. Water 1:52–75

Wagle P, Gowda PH (2019) Editorial for the special issue "Remote sensing of evapotranspiration (ET)". Multidisciplinary Digital Publishing Institute

Wei W, Zhang J, Zhou J, Zhou L, Xie B, Li C (2021) Monitoring drought dynamics in China using optimized meteorological drought index (OMDI) based on remote sensing data sets. J Environ Manag 292:112733

Wells N, Goddard S, Hayes MJ (2004) A self-calibrating Palmer drought severity index. J Clim 17(12):2335–2351

Wen W, Timmermans J, Chen Q, van Bodegom PM (2021) A review of remote sensing challenges for food security with respect to salinity and drought threats. Remote Sens 13(1):6

Yong B, Chen B, Tian Y, Yu Z, Hong Y (2016) Error-component analysis of TRMM-based multi-satellite precipitation estimates over mainland China. Remote Sens 8(5):440

Zhang A, Ji Y, Sun M, Lin C, Zhou P, Ren J, Luo D, Wang X, Ma C, Zhang X (2021) Research on the drought tolerance mechanism of Pennisetum glaucum (L.) in the root during the seedling stage. BMC Genom 22(1):1–14